euspen's 24th International Conference & Exhibition, Dublin, IE, June 2024

www.euspen.eu

Advanced camera calibration for lens distortion correction in hybrid manufacturing processes: An exemplary application in laser powder bed fusion (PBF-LB/M)

B. Merz[1,2], K. Poka[1], G. Mohr[1], K. Hilgenberg[1], J. Polte[2,3]

[1]*Additive Manufacturing of Metallic Components, Bundesanstalt für Materialforschung und –prüfung (BAM), Berlin, Germany*
[2]*Institute for Machine Tools and Factory Management IWF, Technische Universität Berlin, Berlin, Germany*
[3]*Fraunhofer Institute for Production Systems and Design Technology IPK, Pascalstraße 8-9, 10587 Berlin, Germany*

Benjamin.Merz@bam.de

Abstract

Hybrid additive manufacturing is becoming increasingly important in the field of additive manufacturing. Hybrid approaches combine at least two different manufacturing processes. The focus of this work is the build-up of geometries onto conventionally manufactured parts using Powder Bed Fusion with Laser Beam of Metals (PBF-LB/M). The hybrid build-up requires a precise position detection system inside the PBF-LB/M machines to determine the exact position of the existing component. For this purpose, high-resolution camera systems can be utilized. However, the use of a camera system is associated with several challenges. The captured images are subject to various distortions of the optical path. Due to these distortions, it is not possible to use the images for measurements and, therefore, it is not possible to calculate the positions of objects. In this study a homography matrix is calculated to correct keystone distortion in the images. Different calibration patterns have been tested for the calculation of the homography matrix. The influence of the number of calibration points on the precision of position detection of objects is determined. Furthermore, the influence of an additional camera calibration by using ChArUco boards is evaluated. The result is a camera calibration workflow with associated calibration pattern for a precise position detection of parts inside PBF-LB/M machines allowing a hybrid build-up with minimum physical offset between base component and build-up.

Keywords: Additive manufacturing, hybrid build-up, position detection, camera calibration

1. Introduction

One possible application of hybrid additive manufacturing (AM) is the build-up of geometries onto existing components [1,2]. Powder bed usion of metals utilizing a laser beam (PBF-LB/M) can be used to achieve a precise build-up with minimal offset between the component and the AM structure to avoid subsequent machining. Standard PBF-LB/M machines are not designed to build-up onto existing components. For this reason, the position of the mounted component has to be determined with high accuracy and precision. A high resolution camera system can be used to achieve this [3].

Images acquired by camera systems are subject to different levels of distortion. Lens distortion is primarily caused by the inherent imperfections in the design and manufacturing of camera lenses. This type of distortion manifests as either barrel distortion, where straight lines appear curved outward, or pincushion distortion, where straight lines seem to curve inward [4]. It can be corrected utilizing a camera matrix, which can be calculated by using ChArUco boards [5]. CharUco boards combine the traditional chessboard pattern with binary matrix markers, similar to QR codes, called ArUco markers, thereby improving calibration accuracy and robustness for calculation of the camera matrix. The position of the camera is off-axis to the component whose position has to be detected, resulting in a keystone distortion in the image. This type of distortion manifests that straight parrallel lines in real world converge or diverge on the projection displayed in the image. A homography matrix can be utilized to correct this distortion and transform the component position into the machine coordinate system [3,6]. In this paper, the influence of the number of calibration points for the calculation of the homography matrix is determined. Subsequently, the influence of a simultaneous correction of the lens distortion correction by using ChArUco boards is analyzed.

2. Experimental Setup

The setup for position detection is integrated in the commercial PBF-LB/M machine SLM 280 HL, SLM Solutions Group AG, Germany. The high resolution camera is a monochrome VLXT-650M.I, Baumer Holding AG, Switzerland with a resolution of 65.4 MPixel in combination with the modular lens system Apo-Componon 4.5/90, Jos. Schneider Optische Werke GmbH, Germany with a focal length of 90 mm. The camera is mounted outside the build chamber by using a tilt-shift-adapter to avoid vignetting effect. This setup results in a field of view (FOV) of approx. 160 x 120 mm² and an idealised spatial resolution of 17.2 µm/pixel [7]. The experimental setup is shown in Figure 1.

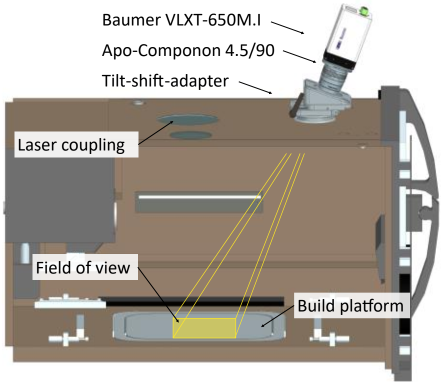

Figure 1. Experimental setup in SLM 280HL [7]

3. Accuracy and precision of calibration method

3.1. Influence of homography matrix

The calculation of a homography matrix is required to compensate keystone distortion in perspective distorted images. It is calculated by superimposing real source and ideal target points. The calibration points are generated by engraving reference markers on a black calibration plate with the laser of the PBF-LB/M machine. For calculation of the homography matrix, four different patterns with 5, 25, 169 and 529 reference markers are engraved by the laser. The calibration points are arranged symmetrically around a center point. This results in a grid of reference points with constant pitch between the points. The calibration pattern with 25 reference points is shown as an example in Figure 2. With respect to the 160 x 120 mm² FOV, the marker size is reduced with increasing number of reference points.

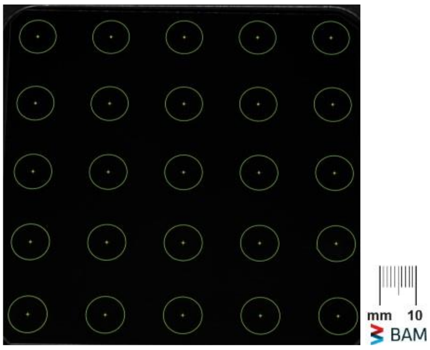

Figure 2. Exemplary image of 25 reference markers calibration pattern with detected marker positions

The coordinates of these ideal points, representing the target points, are known from the CAM system. After engraving the calibration patterns, an image of each pattern is captured by the camera. The real positions of the reference markers on the calibration plate can vary due to systematic errors of the PBF-LB/M process [8]. By directly detecting the reference markers positions in the images, these errors are considered for calculation of the homography matrix. To detect the position of the reference markers, the images are first binarised using a global threshold. After detecting the marker contours using the border following algorithm, the centroid of the markers are determined by the first order image moments [3,9]. These identified positions serve as the pivotal source points essential for the calculation of the homography matrices. In the proposed method, the determination of the target points is based on the positional data of the source points. First, the distances between all the source points are determined seperately along the x- and y-direction. It is known from the CAM system that the distances between points are equal. Consequently, the minimum distance value from these calculations is used to calculate new corresponding points, starting from the center point of the calibration pattern. A schematic representation of the calculated target points using the example of 25 source points is shown in Figure 3. These new corresponding points are the target points essential for the calculation of the homography matrix. By superimposing the determined source points with the calculated target points, the homography matrices for all calibration patterns are calculated.

The influence of the different perspective corrections on the precision and accuracy of the position detection is then determined. For this, a distinct test pattern is engraved onto calibration plates utilizing the laser. Different geometries are engraved to ensure variation in the appearance of the shape in the camera image. A total of seven geometric shapes were engraved three times each at different positions on the calibration plate. The design and layout of the test pattern is shown in Figure 4.

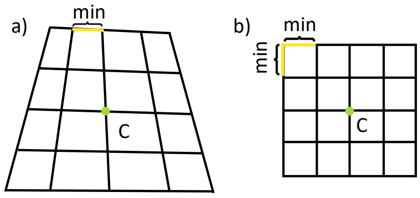

Figure 3. Schematic of target point calculation with highlighted center point a) determined source points from camera images; b) calculated target points based on minimum reference marker distance

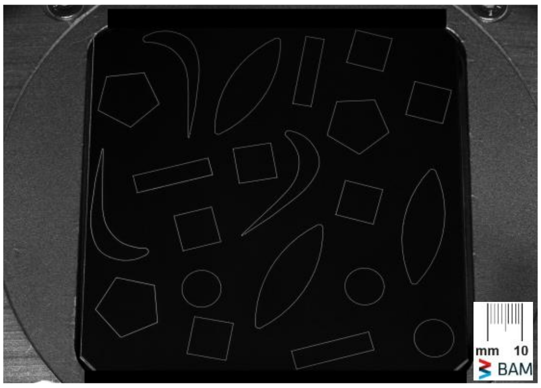

Figure 4. Contrast enhanced image of test pattern

In total the test pattern is engraved 12 times and images are captured. With the 21 geometrical shapes on each plate this results in 252 reference positions for validation of the influence of the number of calibration points to the accuracy and precision of position detection. The keystone distortion in the acquired images is successively corrected using the different homography matrices $\mathbf{H}_{5}$, $\mathbf{H}_{25}$, $\mathbf{H}_{169}$ and $\mathbf{H}_{529}$, where the indeces correspond to the number of calibration points. From each perspective corrected image, the positions of the objects are determined using the workflow described above. The deviations between the ideal positions derived from the CAD system and the determined positions are calculated. The deviation is calculated separately for the x- and y-direction. The results are shown in Figure 5.

It is observed that the dispersion of values along the y-axis is more pronounced compared to the x-axis. Furthermore, an increase in the number of calibration points is associated with a larger deviation from the ideal values. Notably, more calibration points also results in a shift of the deviations towards the negative x-direction. This is evidenced from the accuracy of the mean values, which otherwise indicate a systematic offset. The reason for this can be found in small installation inaccuracies of the camera, which cause a stronger perspective in the negative x-direction, which is amplified by additional calibration points.

The descriptive statistics, shown in Figure 5, confirm the observations made. The standard deviations for all perspective corrections are within a similar range. This indicates a similar level of precision across the various rectifications of keystone distortion. Notably, the standard deviation in the y-direction is at least twice as large as that in the x-direction. As Figure 1 illustrates the machine setup, it can be seen that the camera is aligned centrally in the x-direction. To capture relevant areas of the build platform, the camera is tilted around the x-axis. This leads to a more pronounced perspective distortion in the y-direction, resulting in a larger residual deviation after keystone correction. This is reflected in the higher standard deviation observed in the y-direction.

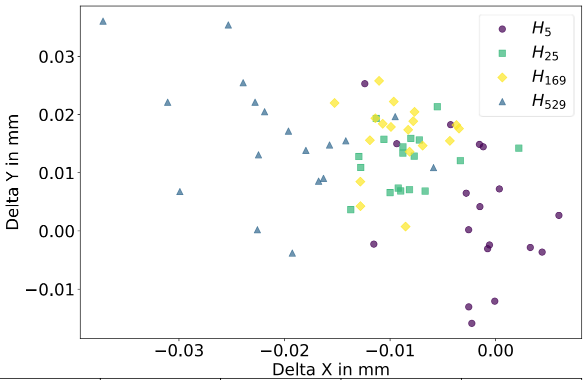

	$mean_X$	σ_X	$mean_Y$	σ_Y
H_5	-0.0051	0.0184	-0.0038	0.0469
H_{25}	-0.0113	0.0174	0.0068	0.0456
H_{169}	-0.0123	0.0176	0.0105	0.0461
H_{529}	-0.0233	0.0182	0.0093	0.0471

Figure 5. Deviation and scatter of values for keystone correction using different homography matrices (outlier corrected)

The smallest deviations from the mean values to the ideal values can be observed by correction of the keystone distortion using the homography matrix $\mathbf{H_5}$. The deviation is - 0.0052 mm in the x-direction and - 0.0038 mm in the y-direction. The result indicates, that a higher number of calibration points is associated with a less accurate compensation of keystone distortion. To support this hypothesis, statistical significance was assessed via p-values, and effect sizes were quantified using Cohen's d. As depicted in Table 1, both the x-direction and y-direction exhibit low p-values with a significane level below 0.05, stating a statistically significant difference in perspective correction accuracy between $\mathbf{H_5}$ and the other corrections, with a moderate effect size denoted by Cohen's d. This validates the hypothesis that a greater number of calibration points results in reduced precision in correcting keystone distortion.

Table 1 Statistical significance of the observed deviations (p-value) and effect size (Cohen's d).

	Cohen's d_X	p-value$_X$	Cohen's d_Y	p-value$_Y$
$\mathbf{H_5}$ to $\mathbf{H_{25}}$	0,3327	2.09e-04	-0,22275	1.27e-02
$\mathbf{H_5}$ to $\mathbf{H_{169}}$	0,3845	1.91e-05	-0,29935	8.38e-04
$\mathbf{H_5}$ to $\mathbf{H_{529}}$	0,9545	2.92e-24	-0,27232	2.36e-03

One possible reason for this is that increasing the number of calibration points leads to overfitting the perspective distortion in one plane. In addition, the size of the reference markers becomes smaller as their number increases, making them more susceptible to errors during image processing. These errors compromise the accuracy of position detection via image moments, leading to incorrect estimations of the minimum distance between source points. Therefore, the target point grid is inaccurately determined (see Figure 3), which eventually affects the calculation of the homography matrix.

The results indicate that utilizing 5 reference points for perspective correction significantly enhances accuracy. Therefore, it can be concluded that rectification utilizing a homography matrix calculated from 5 calibration points is sufficient.

3.2. Influence of camera matrix

Additional lens distortion correction can improve the accuracy, precision and robustness of the camera calibration process [10, 11]. Lens distortion can be corrected by calculating the camera intrinsic parameters, summarised in the camera matrix $\mathbf{C}$. To calculate the camera matrix, it is necessary to have reference images of a known object. ChArUco boards can be used for this purpose [5]. For accurate computation of the camera matrix, a dataset of 30 images featuring a ChArUco board is captured, with a focus on ensuring a high variability in the orientations of the ChArUco board within these images. This data set is used to calculate the camera matrix $\mathbf{C_0}$.

The influence of simultaneously correcting lens distortion and perspective distortion is validated using the same set of 12 images featuring the test pattern with 21 geometric shapes. Lens distortion and keystone distortion are corrected in the images. The positions of the test objects are then determined using the workflow described above. The deviations between the ideal positions derived from the CAD system and the determined positions are calculated. The deviations are calculated separately for the x-and y-directions. For reference, the results of correcting only keystone distortion by $\mathbf{H_5}$ are shown. The result is shown in Figure 6.

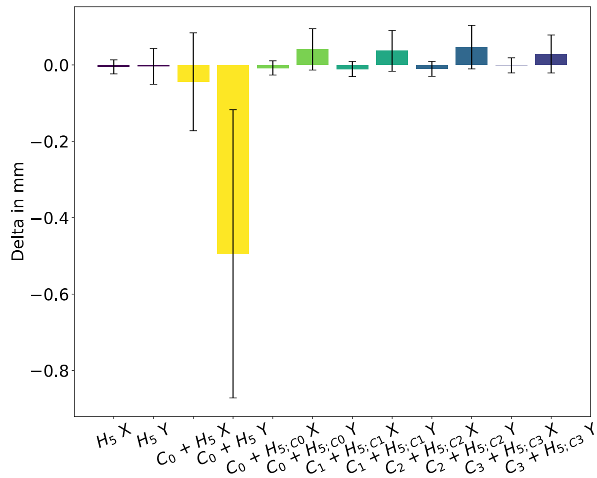

	$mean_X$	σ_X	$mean_Y$	σ_Y
H_5	-0.0051	0.0184	-0.0038	0.0469
$C_0 + H_5$	-0.0442	0.1282	-0.4945	0.3772
$C_0 + H_{5;C0}$	-0.0079	0.0186	0.0407	0.0542
$C_1 + H_{5;C1}$	-0.0106	0.0197	0.0368	0.0534
$C_2 + H_{5;C2}$	-0.0103	0.0195	0.0465	0.057
$C_3 + H_{5;C3}$	-0.0012	0.0198	0.0286	0.0497

Figure 6. Deviation between ideal and determined positions after different distortion corrections

In the initial test, lens distortion is corrected by $\mathbf{C_0}$, followed by keystone distortion using $\mathbf{H_5}$. Compared to the reference, a significant increase in both mean values and standard deviations is observed. This may be due to the fact that the homography matrix $\mathbf{H_5}$ is calculated from an image subject to lens distortion. Consequently, the projective transformation between the source points and target points does not align correctly, resulting in an inaccurate calculation of the homography matrix. Such miscalculation leads to larger deviations and increased scatter from the nominal values. For this reason, the lens distortion is corrected in the input image before calculating the homography matrix, resulting in the new matrix $\mathbf{H_{5;\,C0}}$. The lens distortion in the 12 test images is then corrected by $\mathbf{C_0}$, followed by compensation of the keystone distortion using $\mathbf{H_{5;\,C0}}$. This approach improves accuracy and precision, but it does not reach the accuracy level of corrections using $\mathbf{H_5}$ alone. A potential reason for this is that the corner points of the ChAruCo boards in set of 30 images are not recognized with sufficient accuracy, leading to inaccuracies when calculating the camera matrix.

To minimize inaccuracies in detecting ChArUco boards, various methods for refining the detection of corner locations within the ArUco marker are examined. The different methods subpix, contour and AprilTag from the OpenCV library are applied for corner refinement [12, 13]. The subpix method is refining the corner locations with subpixel accuracy. The contour method is fitting lines to the detected contour points. The AprilTag method is using the improved AprilTag 2 decetion algorithm [12,13].

Based on the refined detection of the ChArUco boards, the three new camera matrices $\mathbf{C}_1$ for subpix refinement, $\mathbf{C}_2$ for corner refinement and $\mathbf{C}_3$ for AprilTag refinement are calculated. These matrices are then utilized to correct the lens distortion in the input images for calculation of the new homography matrices subpix ($\mathbf{H}_{5;\,C1}$), corner ($\mathbf{H}_{5;\,C2}$) and AprilTag ($\mathbf{H}_{5;\,C3}$). For evaluation, the lens distortion in the 12 test images is corrected using the new camera matrices, followed by the correction of keystone distortion using the new homography matrices.

With the subpix refinement, the standard deviation of the values can be reduced compared to the results of no correction. The accuracy in the x-direction decreases, while the accuracy in the y-direction increases. The results can not be further improved by the method contour refinement. An improvement in accuracy can be achieved using the AprilTag refinement. Compared to the other refinements, the deviations are reduced in both the x- and y-direction. The standard deviation in the y-direction can be improved, while the standard deviation in the x-direction increases slightly. The reason for the improvement of the AprilTag method is that 12 more ArUco markers are detected in the images due to the corner refinement. As a result, the accuracy of lens distortion correction can be increased.

Compared to the $\mathbf{H}_5$ reference method, which only corrects keystone distortion, the precision in the x-direction improves from - 0.0051 mm to - 0.0012 mm. In the y-direction, the AprilTag method, with an mean value of 0.0286, is about 7 times lagerer than the $\mathbf{H}_5$ reference. There is also a slight increase in the standard deviation. In all cases, the deviation of the mean values can only be improved in one direction. Simultaneous enhancement of both the x- and y-directions, in terms of mean values and standard deviations, cannot be attained through additional correction of lens distortion. One potential reason for this is the accuracy of the ChArUco board, which was printed at a resolution of 1200 dpi using a laser printer, equivalent to a dot resolution of approx. 0.0212 mm. Consequently, the inherent error margin in the ChArUco board exceeds the spatial resolution of the camera system. These inherent errors lead to an inaccurate calculation of the camera matrix. Given the wide variability in the 30 images used for the camera matrix calculation, these inaccuracies impact all directions. Hence, no consistent improvement trend is observed in both the x-direction and y-direction simultaneously.

4. Conclusion

In this paper, the influence of different distortion corrections in images on the accuracy and precision of position detection for the hybrid build-up using PBF-LB/M is investigated. An imprecise calibration of the camera can lead to errors in detecting objects within the process chamber of the PBF-LB/M machine. It is important to keep this error as small as possible to ensure the smallest possible offset between the component and the AM structure. Large offsets can be particularly disadvantageous when building fine structures, for which the PBF-LB/M process is particularly advantageous. Depending on the size of the structures built, even small offsets can lead to waste or compromise process stability. Additionally, reworking internal surfaces or cavities of hybrid parts may be difficult or not possible. For components with internal cooling channels, an offset may reduce the flow quality of the coolant, which could compromise its intended purpose.

The influence of correction of keystone distortion is analyzed using calibration patterns with 5, 25, 169 and 529 reference markers. These markers were engraved on calibration plates using the laser of the PBF-LB/M machine. The positions of the reference markers were detected through image processing to calculate the homography matrices. The accuracy and precision of perspective correction on the position detection of objects is evaluated by validating them using 12 test images. The best results are found with the calibration of 5 reference points. One possible reason for this could be that the reference markers become smaller as their number increases, making them more susceptible to errors during image processing. This leads to an incorrect calculation of the homography matrix.

The effect of additional calibration for lens distortion is also examined. The camera matrix is derived from 30 images of a ChArUco board. The accuracy and precision of position detection are evaluated using the same set of 12 test images, where lens distortion is corrected first, followed by keystone distortion correction. The calibration of lens distortion did not result in significant improvement compared to correcting keystone distortion alone. This might be attributed to the inherent errors in the ChArUco board used for calibration, leading to a flawed camera matrix calculation for lens distortion correction.

The high-performance APO-COMPONON 4.5/90 lens used exhibits very low lens distortion, particularly in the center of the image, which is the region of interest. Additional correction of lens distortion does not significantly improve the already minimal distortion in this area. Although a slight improvement in accuracy in the x-direction can be achieved by the additional correction of lens distortion using the AprilTag method, the correction from the perspective with 5 reference points is considered to be sufficient.

The transfer of camera calibration to the hybrid build-up of real components has been demonstrated on single demonstrator geometries [3,7] and will be the subject of future investigations on a larger scale.

References

[1] Popov, V. V.; Fleisher, A.: Hybrid additive manufacturing of steels and alloys. Manufacturing Review **7** (2020).

[2] Andersson, O.; Graichen, A.; Brodin, H.; Navrotsky, V.: Developing Additive Manufacturing Technology for Burner Repair. Journal of Engineering for Gas Turbines and Power **139** (2017).

[3] Merz, B.; Nilsson, R.; Garske, C.; Hilgenberg, K.: Camera-based high precision position detection for hybrid additive manufacturing with laser powder bed fusion. Int J Adv Manuf Technol **125** (2023).

[4] Neale, W. T.; Hessel, D.; Terpstra, T.: Photogrammetric Measurement Error Associated with Lens Distortion. SAE 2011 World Congress & Exhibition (2011).

[5] An, G. H.; Lee, S.; Seo, M.-W.; Yun, K.; Cheong, W.-S.; Kang, S.-J.: Charuco Board-Based Omnidirectional Camera Calibration Method. Electronics **7** (2018)

[6] Lee, J.-Y.: Robust Camera Calibration with a Single Image by Planar Homography. Proceedings of the 18th IEEE Int. Conference on Advanced Video and Signal Based Surveillance, Madrid (2022).

[7] Merz, B.; Poka, K.; Mohr, G.; Hilgenberg, K.: Precise Position Detection for Repair of Gas Turbine Blades using PBF-LB/M. Proceedings of the 5th International Symposium Additive Manufacturing ISAM (2023).

[8] Gradl, P. R.; Tinker, D. C.; Ivester, J.; Skinner, S. W.; Teasley, T.; Bili, J. L.: Geometric feature reproducibility for laser powder bed fusion (L-PBF) additive manufacturing with Inconel 718. Additive Manufacturing **47** (2021).

[9] Suzuki, S.; Abe, K.: Topological structural analysis of digitized binary images by border following. Computer Vision, Graphics, and Image Processing **30** (1985).

[10] Gao, D.; Yin, F.: Computing a complete camera lens distortion model by planar homography. Optics & Laser Technology **49** (2013).

[11] Rudakova, V.; Monasse, P.: Camera Matrix Calibration Using Circular Control Points and Separate Correction of the Geometric Distortion Field. Proceedings of the Canadian Conference on Computer and Robot Vision (2014).

[12] Bradski, G.: The OpenCV Library. Dr. Dobb's Journal of Software Tools (2000).

[13] Wang, J.; Olson, E.: AprilTag 2: Efficient and robust fiducial detection. Proceedings of the IEEE/RSJ International Conference on Intelligent Robots and Systems (IROS) (2016).